A&A 526, A150 (2011)
DOI: 10.1051/0004-6361/201015724

Astronomy & Astrophysics

Near-infrared SOAR photometric observations of post common envelope binaries⋆

T. Ribeiro and R. Baptista

Departamento de Física, Universidade Federal de Santa Catarina, Campus Trindade, 88040-900 Florianópolis, SC, Brazil
e-mail: tiago@astro.ufsc.br

Received 8 September 2010 / Accepted 19 November 2010

ABSTRACT

Context. From a number of known post common envelopes binaries (PCEB) only a handful have yet been observed at near-infrared (NIR) wavelengths, and even fewer have modeled NIR light curves. At shorter wavelengths one has access to the cooler and larger components of these systems and has a chance to detect emission from its faint and heavily irradiated atmospheres.
Aims. By modeling NIR light curves of PCEBs, we intend to constrain their system parameters and study the properties of the system components.
Methods. Here we present simultaneous NIR JHK_s light curves of two PCEBs obtained with the 4 m SOAR telescope.
Results. KV Vel and TW Crv are long-period (P_{orb} = 8.6 h and 7.9 h, respectively) PCEBs with strong irradiation effects. The results of light-curve fitting provided solutions with inclination $i = (47 \pm 5)^\circ$, mass ratio $q = 0.3 \pm 0.1$, and radius of the secondary $R_2/a = 0.24^{+0.05}_{-0.03}$ (where a is the orbital separation) for KV Vel, and $i = (42 \pm 9)^\circ$, $q = 0.28 \pm 0.04$, and $R_2/a = 0.22 \pm 0.01$ for TW Crv, respectively. For KV Vel, we obtain an average value for the albedo of the secondary star of $\alpha = 0.43$, consistent in the J, H and K_s band. For TW Crv, on the other hand, we obtain values of $\alpha_J = (0.4 \pm 0.1)$ for the J and $\alpha_H = (0.3 \pm 0.1)$ for H-band.

Key words. binaries: close – stars: fundamental parameters – ephemerides – binaries: spectroscopic – subdwarfs

1. Introduction

Cataclysmic variables (CVs) are binary systems where a low-mass dwarf (LMD) star overfills its Roche lobe and transfers matter to a more massive white dwarf (WD) at mass transfer rates typically of $\dot{M} \sim 10^{-10}$–10^{-8} $M_\odot\,\mathrm{yr}^{-1}$. Since the orbital separation (and the Roche lobe) is expected to increase when a lower mass star transfers matter to a more massive one (see Hellier 2001, for an overview), the binary must continuously lose angular momentum to sustain mass transfer. CVs are thought to be the remnants of initially wide, detached binaries where the more massive star evolves to a giant and expels its outer layers through a common-envelope (CE) configuration leaving a detached LMD+WD system. A detailed description of this evolutionary picture is given by Tappert et al. (2007).

Recently, a series of efforts have been made to unveil the evolutionary picture of CVs i.e., its angular-momentum loss history. Although there are alternative models, Kolb et al. (1998) concluded that the disrupted magnetic braking model (DMB) is the most plausible explanation for CV evolution. Since the secondary star is responsible for the magnetic braking mechanism, understanding its properties is essential for developing the DMB theory. By studying the secondary stars of pre-CVs and PCEBs we are able to access stars in the same regime as those of CVs without the accretion complexity.

To that end, we have collected near-infrared (NIR) JHK_s light curves of a sample of PCEBs covering a range of orbital periods from around the period gap ($P_{orb} \sim 2$–3 h) up to $P_{orb} \sim 8$ h, the largest orbital period suitable for full coverage within one night of (ground) observation. This paper reports the results of the analysis of data from two of these systems. The observations and data reduction are presented in Sect. 2. Sample selection criteria and specific information about the objects of this study are given in Sect. 3. By modeling the light curve of these systems we are able to put constraints on their orbital system parameters and, from the colors of each component, study their properties. In Sect. 4 we present the data analysis and discuss of each target separately. Conclusions and further perspectives are presented in Sect. 5.

2. Observations and reduction

All observations were performed in queue mode with the 4.1 m SOAR Telescope at Cerro Pachon, Chile, using the OSIRIS Infrared Imager and Spectrograph (Pogge et al. 1999) in imaging mode. A summary of the observations is presented in Table 1, where t_{exp} is the exposure time and *ndith* is the number of dithering positions. All runs were carried out under nonphotometric conditions, with thin clouds and cirrus, resulting in variable sky transparency. Nevertheless, none of the observations had to be interrupted due to bad weather.

Time series of NIR photometry were performed quasi-simultaneously in J, H, and K_s, except in cases where the system was too faint and/or had too short orbital period so that it was not possible to obtain good signal-to-noise data within the constraints given by the exposure time and the minimum time resolution. The procedure of quasi-simultaneous photometry is basically to perform a set of acquisitions in one filter, change to the next filter, perform another set, and so on. This method guarantees that any feature that lasts longer than an acquisition cycle will be present in all light curves.

⋆ The near-infrared photometric data can be retrieved at the CDS via anonymous ftp to cdsarc.u-strasbg.fr (130.79.128.5) http://cdsarc.u-strasbg.fr/viz-bin/qcat?J/A+A/526/A150

Table 1. Journal of observations.

Target name	Date of observation	Bands	t_{exp} J	H	K_s	*ndith*
KV Vel	2007-03-24	JHK_s	10 s	10 s	20 s	5
TW Crv	2007-04-24	JH	10 s	20 s	–	6

In some cases, the required total exposure time to achieve the desired signal-to-noise ratio (S/N) saturated the profile of the target or of a field comparison star. In these cases we had to split a single exposure into more than one, and the final image is the sum of *NC* coadd images. For the targets discussed in this paper, the exposure time were short enough that no coadd procedure was necessary.

Data reduction was performed using IRAF[1]. All frames were first trimmed, and the nonlinearity of the detector was corrected by employing the third-order polynomial solution of Pogge et al. (1999) for the OSIRIS instrument. The frames were then divided by the normalized flat-field. A bad pixel mask was constructed from flat-field images and used to correct for bad pixels. Since the sky contribution to NIR light is considerably high, it is standard to perform a dithering procedure, nodding the telescope into *ndith* different positions after each image is acquired. The sky level is obtained by taking the median of the *ndith* image. Each image is then iteratively shifted to match a reference image (usually the first image of the night), and aperture photometry is extracted for the target and all possible field stars (at least one star, aside from the target, for each image field is required) using a "variable aperture" (aperture radius = $2 \times FWHM$). The filter was changed after each set of *ndith* acquisitions.

Differential light curves (target star flux divided by comparison star flux) were computed in order to account for sky transparency fluctuations during the night, and flux calibrated from the 2MASS JHK_s magnitudes of the field comparison star and zero point constants (Skrutskie et al. 2006).

3. Sample

We selected a sample of southern PCEBs without accurate NIR light curve models. We searched in the catalog of Kube et al. (2002) for objects with confirmed orbital period of less than an observing night ($P_{orb} \leq 8$ h) and for systems where the exposure time required to achieve $S/N = 50$ is less then $P_{orb}/50/N_{filters}$ (with OSIRIS+SOAR, where $N_{filters}$ is the number of filters to be used for simultaneous photometry). The latter is a requirement for light curve modeling. Since we are interested in secondary stars properties "as-a-star", we did not exclude systems with subdwarf primaries. Some properties of the targets analyzed in this work are presented in Table 2 and discussed below.

3.1. KV Vel

KV Vel (or LSS 2018) is a non-eclipsing binary containing a hot subdwarf primary ($T_1 = 77\,000$ K) and a faint low-mass secondary star, and was the first central object of a planetary nebula discovered to be a double-lined binary (Drilling 1985). Drilling (1985) provided ephemeris, radial velocity measurements, and parameter determination of the system using UBV photoelectric measurements, IUE spectrophotometry, and high-resolution spectroscopy.

Drilling (1985) modeled the UBV light curves of KV Vel considering a simple heating model with spherical stars and no additional flux from the secondary (besides the one produced by heating). Landolt & Drilling (1986) applied the same model to UBVRI light curves of KV Vel and pointed out that the quality of the fit degraded for wavelengths longer than 5500 Å. Beyond this wavelength the secondary star contribution likely becomes significant and its distorted shape could account for the miss-fitting. In that sense, Hilditch et al. (1996) analyzed the same data of Landolt & Drilling (1986) with an improved model that accounted for the secondary flux and distorted shape as well as for illumination and atmospheric (e.g., limb- and gravity-darkening) effects. Although this improved model was able to provide good fit to the data, a problem with the modeling illumination procedure was later reported by Hilditch et al. (2003). After inspecting the previous model, they found a missing factor of π combined with a miss-calculation of the surface normal vector of the emergent flux. These resulted in an underestimation, and possibly misshape, of the reflection effect, leading to unrealistic physical parameters from the fit.

As stated by Landolt & Drilling (1986) and later by Hilditch et al. (1996), modeling of infrared light curves of this binary would be key to our understanding of its properties and of others of its kind, setting our motivation for this analysis.

3.2. TW Crv

TW Crv (or EC11575-1845) is a close binary similar to KV Vel. Both are long orbital period systems containing a hot subdwarf primary and a cool M dwarf secondary. A detailed description of this system was presented by Chen et al. (1995), who provided the first analysis of this close binary, combining $UBVRIJHK$ photometry and optical spectroscopy. Their light curves were used to derive an ephemeris for the system,

$$T_{mid}(E) = 2448661.6049(\pm 3) + 0.32762(\pm 3) \times E, \quad (1)$$

by fitting a sinusoidal curve to determine the time of maximum light. A simple model of irradiated non-emitting spherical secondary, similar to that of Drilling (1985), was used to model its optical light curves. As noted, this model produces a poor fit to NIR light curves, since the assumption of a nonemitting secondary clearly fails at longer wavelengths.

Radial velocity curves of the system were constructed using the C III/N III blend at λ4650 Å, providing velocity semi-amplitudes of $K_1 = (40 \pm 2)$ km s^{-1} and $K_2 = (119 \pm 4)$ km s^{-1} for the primary and for the secondary, respectively (Chen et al. 1995). As Chen et al. (1995) pointed out, the measured K_2 is actually the radial velocity of the irradiated face of the secondary, rather than the velocity of its center of light. They derived equations to correct that effect, as a function of the radius of the star, assuming uniform irradiation.

Exter et al. (2005) report the analysis of high-resolution (1.1 Å), time-resolved spectroscopy for TW Crv. They provided radial velocity measurements for both components of the system yielding values of $K_1 = (53 \pm 2)$ km s^{-1} and $K_2 = (125 \pm 2)$ km s^{-1} for the primary and for the secondary, respectively. As in the case of Chen et al. (1995), the latter is also the radial velocity of the center of light and must be corrected to the center of mass of the star before being used to derive binary parameters.

For this analysis we used new NIR light curves with higher S/N and lower exposure time and an improved model to analyze the data.

[1] IRAF is distributed by the National Optical Astronomy Observatories, which are operated by the Association of Universities for Research in Astronomy, Inc., under cooperative agreement with the National Science Foundation.

Table 2. Properties of sample objects.

name	$P_{\rm orb}[d]$	$K_{\rm s}$	$J-H$	$H-K_{\rm s}$	SP1	SP2
KV Vel	0.36[3]	15.1[3]	−0.116[3]	+0.644[3]	sdOB[4]	M6±1V[4]
TW Crv	0.33[3]	13.3[3]	−0.022[3]	−0.016[3]	sdO[2]	M?V[2]

Notes. Magnitudes were extracted from the 2MASS catalog.

References. [(1)] Kilkenny et al. (1988); [(2)] Chen et al. (1995); [(3)] Skrutskie et al. (2006); [(4)] Drilling (1985).

4. Data analysis

We analyzed the data with the aid of a light curve modeling code similar to the (Wilson & Devinney 1971, hereafter WD) algorithm. The code was developed by us to model the NIR light curves of detached and semi-detached close binaries, according to the routines outlined by Kallrath & Milone (1999). Our code was checked against the WD code and also with the code developed by Watson (2002). It was successfully applied to derive orbital parameters of the CV IP Peg and, by extracting the light curve of the secondary, allowed the application of eclipse mapping techniques to its accretion disk (Ribeiro et al. 2007). In the case of pre-CVs, the surface of the secondary is allowed to be any equipotential within its Roche lobe for a given filling factor, which gives the gravitational potential at the surface of the star with respect to the potential of the Roche lobe ($f_{\rm fac} = \Phi_2/\Phi_{RL1} \geq 1.0$). Thus, a filling factor of unity corresponds to a Roche lobe-filling secondary star, while $f_{\rm fac} > 1.0$ represents underfilling components.

The radiation field of the modeled component is modified to account for gravity- and limb-darkening, as well as for illumination effects. The latter considers a point-like source at the position of the primary star with bolometric irradiation $I_{\rm irr}$. We used the gravity-darkening coefficient of Sarna (1989) for Roche-lobe filling stars with convective envelopes ($\beta = 0.05$). Limb-darkening coefficients are treated when discussing each target separately.

The parameters of the modeling procedure are mass ratio ($q = M_2/M_1$), inclination (i), fluxes of the secondary (F_2) and of the primary (F_1), irradiated intensity ($I_{\rm irr}$) and filling factor ($f_{\rm fac}$). Since we have no a priori information on the orbital separation and/or primary temperature with light curve modeling, we have used $I_{\rm irr}$ to account for the amplitude of the irradiation effect (assuming an albedo of $\alpha = 1.0$) and adopted the orbital separation as our distance scale. Once we know the amount of irradiation, we can discuss its origins. All light curves are modeled simultaneously. For a set of n light curves, q, i, and $f_{\rm fac}$ are common parameters, while F_2, F_1, and $I_{\rm irr}$ are particular to each data set. We proceed by minimizing the χ^2 of the model with respect to the data. The procedure works by first employing a simulated annealing scheme to search for the region of best solution, and then an amoeba minimization routine (Press et al. 1986) is employed to fine-tune the solution. Below we present and discuss the results of the modeling of the data for each target.

4.1. KV Vel

Our NIR light curves of KV Vel (Fig. 1) are largely dominated by reflection effects, and resembles its optical light curves (Hilditch et al. 1996). The amplitude of the reflection effect at NIR is $\Delta H \sim 0.7$ mag against 0.55 mag in the V band.

We fitted separate sinusoids to the $JHK_{\rm s}$ data in order to measure the time of maximum light. The symmetric shape of the orbital hump with respect to the phase of maximum

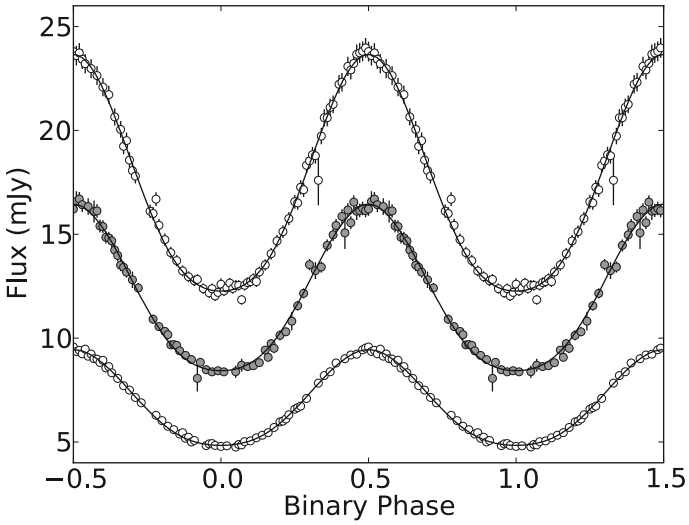

Fig. 1. Orbital light curves of KV Vel, from top to bottom in J, H and $K_{\rm s}$ bands, respectively. Model light curves are overploted as solid lines. The light curves are repeated in phase for better visualization.

indicates that it is produced by uniform irradiation of the secondary star by a source centered on the position of the primary star. In this case, we expect that the maximum of the light curve coincides with binary phase $\phi = 0.5$, where the observer looks directly at the irradiated face of the secondary star. However, if we phase-fold the data according to the ephemeris of Kilkenny et al. (1988), the maximum light is displaced from its expected phase by $\Delta\phi \sim 0.01$. The discrepancy cannot be accounted for by the uncertainty in the ephemeris of Kilkenny et al. (1988).

We, therefore combined our measured time of maximum with those of Drilling (1985), Landolt & Drilling (1986), and Kilkenny et al. (1988, see Table 3) to compute a revised ephemeris for KV Vel. The best fit least-squares revised linear ephemeris is

$$T_{\rm max} = {\rm HJD}\ 2\,445\,834.5174(\pm4) + 0.3571205(\pm5)\,E, \qquad (2)$$

where E is the cycle number. The standard deviation of the data with respect to this ephemeris is $\sigma = 9.85 \times 10^{-3}$, for a reduced chi-square of $\chi^2_\nu = 1.32$. The (O–C) values with respect to this revised ephemeris are listed in Table 3.

Although the revised linear ephemeris provides a nice fit to our data, it yields a poor fit to the data of Kilkenny et al. (1988). These deviations prompted us to check whether a quadratic ephemeris provides a better fit to the whole data set. We applied the F-test proposed by Pringle (1975) in order to determine the statistical significance of adding an additional term to the linear ephemeris. For this case we obtain $F(1,6) = 2.8$, with a statistical significance lower than 85% for the quadratic ephemeris. We conclude that there is presently no evidence of period changes in KV Vel.

We used the previous determination of secondary star properties (Hilditch et al. 1996) to select square-root limb-darkening

Table 3. Times of maximum light and O–C residuals for KV Vel, where our cycle timings are the mean of individual measurements of the JHK_s bands.

cycle	T(max) (2400000+)	(O–C)[a]	(O–C)[b]	Ref.
−106	45796.671	+0.0084	−0.0019	1
0	45834.52803	+0.0106	+0.0011	2
3	45835.59908	+0.0103	+0.0009	2
829	46130.5735	+0.0032	−0.0000	2
2834	46846.5850	−0.0118	−0.0000	3
2845	46850.5130	−0.0122	−0.0003	3
3018	46912.2940	−0.0130	+0.0002	3
23382	54184.53287	+0.0045	−0.0092	4

Notes. [(a)] With respect to the linear ephemeris of Eq. (2). [(b)] With respect to the linear ephemeris of Landolt & Drilling (1986).

References. (1) Drilling (1985); (2) Landolt & Drilling (1986); (3) Kilkenny et al. (1988); (4) This work.

Table 4. Inferred parameters of KV Vel.

Fluxes of the different components.			
	J	H	K_s
F_2(mJy)	0.40 ± 0.02	0.48 ± 0.1	0.41 ± 0.02
F_1(mJy)	11.4 ± 0.2	7.6 ± 0.1	4.2 ± 0.1
I_{irr}	26.6 ± 0.2	15.6 ± 0.1	10.1 ± 0.1
Simultaneously fitted parameters:			
$i = (47 \pm 5)^\circ$ $q = (0.3 \pm 0.1)$ $f_{fac} = (1.09 \pm 0.02)$[a]			

Notes. [(a)] The filling factor ($f_{fac} = \Phi_2/\Phi_{RL1} \geq 1.0$) is the relative gravitational potential at the stellar surface.

coefficients from Claret (1992). The final set of parameters that best describe our data are shown in Table 4, and the corresponding light curves are shown in Fig. 1. Error estimation was performed through a Monte-Carlo simulation.

Combining the inferred inclination with the radial velocity measurements of Hilditch et al. (1996), we obtain masses of $M_1 = (0.7 \pm 0.2)\,M_\odot$ and $M_2 = (0.3 \pm 0.1)\,M_\odot$ and an orbital separation of $a = (2.1 \pm 0.3)\,R_\odot$. Our inferred inclination is slightly lower than that of Hilditch et al. (1996), leading to higher masses for both components. The inferred filling factor yields a radius[2] of $r2 = 0.24^{+0.05}_{-0.03}$ or $R_2 = 0.50^{+0.07}_{-0.05}\,R_\odot$ for the secondary star. As noticed by Hilditch et al. (1996) and underscored by our measurements, the secondary star of KV Vel is rather oversized for its mass in comparison to isolated main-sequence stars of the same mass – likely an indication that it is out of thermal equilibrium.

The resulting mass for the primary star of KV Vel is only marginally consistent with the canonical mass for subdwarf stars ($M_{sdO} = 0.47\,M_\odot$; Han et al. 2003). The standard scenario proposed by Han et al. 2003 also predicts the formation of stars with masses ranging from $0.3\,M_\odot$ to $0.8\,M_\odot$. In this regard, the primary star of KV Vel may correspond to the rare case of the high-mass end of the predicted subdwarf distribution. Nevertheless, we point out that the radial velocity measurements of KV Vel, from Hilditch et al. (1996), are potentially problematic. For instance, the lack of detailed modeling of the irradiation effect may conceivable hide important systematic errors. Therefore, further radial velocity measurements, with proper modeling of irradiation, are required to solve this issue.

[2] here we list $r2 = R_2/a$, the radius of the secondary in units of the orbital separation

We used the NIR colors of the low-mass component of the binary to investigate its atmospheric properties and to constraint the distance to the system. The NIR colors for the secondary star of KV Vel are consistent with that of an M6V-M5V dwarf star and with those of a black body radiator with temperature $T_{bb} = (3000 \pm 100)$ K. Combining the colors and the radius of the star, we inferred a distance of $d = (680 \pm 60)$ pc to the system. In addition, we also applied the stellar evolutionary models of Baraffe et al. (1998), and consistently obtained a distance of $d = (700 \pm 100)$ pc to the system. The stellar models that provided the best-fit to the NIR flux distribution of the secondary star are those of a star with a mass of $M_2 = 0.2\,M_\odot$ or $M_2 = 0.055\,M_\odot$ and ages of $t = 10^{6.5}$ yr or $t = 10^{8.5}$ yr, respectively.

The resulting model properties of the stellar component are quite controversial. While an age of $10^{8.5}$ yr is in close agreement to what is estimated by Schreiber & Gänsicke (2003), it is quite difficult to reconcile the corresponding low mass of $0.055\,M_\odot$ with the dynamical solution of KV Vel. For example, the discrepancy between the mass and radius of the secondary star would be even more pronounced and harder to explain. On the other hand, although a stellar component with $0.2\,M_\odot$ agrees more closely with our dynamical solution, it is hard to reconcile the corresponding $10^{6.5}$ yr age with the evolutionary stage of a PCEB. However, one might argue that, since the binary has recently evolved from a common envelope phase, the secondary star is still out of thermal equilibrium (which is also indicated by the large radius discrepancy), and therefore, its properties resemble those of young stellar atmospheres. We conclude that the $M_2 = 0.2\,M_\odot$ is the most plausible solution.

4.2. TW Crv

The light curves of TW Crv are also dominated by reflection effect, similar to those of KV Vel. Therefore, the analysis of its NIR light curve is similar to the analysis of KV Vel. We initially phase-folded the data using the ephemeris of Eq. (1). As in the case of KV Vel, the orbital minimum does not occur at phase $\phi = 0$ as expected, but rather at $\phi = -0.13$ (earlier than expected). This is not surprising given the relatively low precision of the ephemeris of Chen et al. (1995) and the long time span between their observations and ours. In analogy to the previous section, we fitted a sinusoid to the light curve to measure the time of minimum light, and combined the new timing with those of Chen et al. (1995) to revise the ephemeris of TW Crv.

The best fit least-squares revised linear ephemeris for TW Crv is

$$T_{min}(E) = 2448661.6049(\pm 3) + 0.3276074(\pm 2)\,E. \quad (3)$$

The results of the light curve fitting analysis are listed in Table 5 and shown in Fig. 2. The filling factor leads to a radius of $r_2 = 0.22 \pm 0.01$ for the secondary star which, using Eq. (5) of Chen et al. (1995), gives a mass ratio of $q = 0.30 \pm 0.01$, in good agreement with our light curve fitting value.

Using Eq. (4) of Chen et al. (1995), together with our values of i and r_2, we obtain $M_T = (0.6 \pm 0.1)\,M_\odot$ for the total mass of the system, $M_1 = (0.5 \pm 0.1)\,M_\odot$ and $M_2 = (0.2 \pm 0.1)\,M_\odot$ for the stellar component masses, and an orbital separation of $a = (1.7 \pm 0.1)\,R_\odot$. The same calculations, which were performed with the radial velocities provided by Exter et al. (2005), result in a total mass of $M_T = (0.9 \pm 0.1)\,M_\odot$, $M_1 = (0.66 \pm 0.05)\,M_\odot$ and $M_2 = (0.24 \pm 0.05)\,M_\odot$ for the stellar component masses. In addition, we obtain an orbital separation of $a = (1.9 \pm 0.1)\,R_\odot$ and a radius for the secondary star of $R_2 = (0.4 \pm 0.1)\,R_\odot$. These

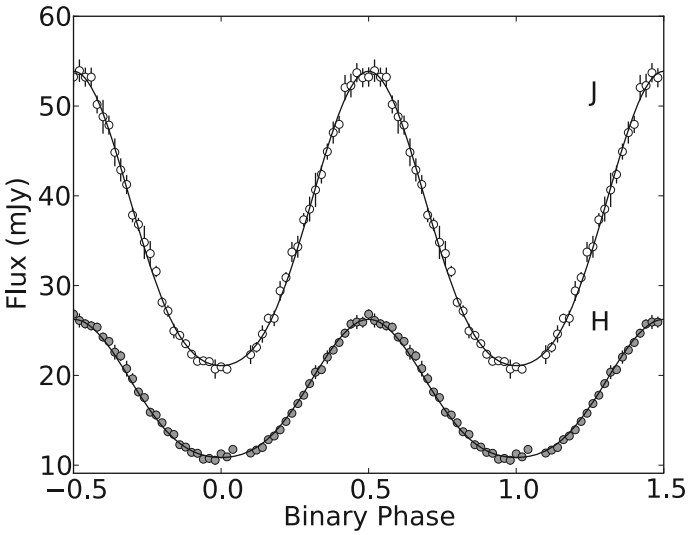

Fig. 2. Light curves of TW Crv in J and H with the corresponding model fits (solid lines). The data were doubled in phase for better visualization.

results are obtained by applying the same correction to K2 as in the case of the Chen et al. (1995) results.

Given the discrepancies between the results using the radial velocity values of Chen et al. (1995) and Exter et al. (2005), it seems that the corrections derived by Chen et al. (1995) do not apply to the data of Exter et al. (2005). For instance, a non-negligible contribution from the underlying secondary star to the narrow emission lines used by Exter et al. (2005) invalidates the procedure. A detailed modeling of the impact of irradiation on the line shape may be necessary to clarify this issue.

The radius of the secondary star obtained from the previous analysis indicates that the secondary star is significantly oversized for its mass. In addition, the flux ratio $(F_2(J)/F_2(H))$ of the secondary star is consistent with a black body of $T \sim 4500$ K at a distance of $d \sim 420$ pc.

5. Discussion and conclusions

New NIR photometry of two long-period PCEBs, KV Vel and TW Crv, was presented and discussed. By measuring times of maximum light of KV Vel and TW Crv, we were able to improve the system ephemerides.

Figures 1 and 2 show our flux-calibrated phase-folded data, together with the corresponding model light curves. The model accounts for both the constant contribution of the primary[3] and of the illuminated distorted secondary, and also for inhomogeneities due to atmospheric effects in the irradiation field of the secondary. We were able to model the NIR light curves leading to well-constrained system parameters (Tables 4 and 5).

From our light curve analysis, it is also possible to investigate the irradiation effect on the secondary surface. In contrast to the standard procedure usually adopted for albedo modeling on these kind of binaries (p. ex., Hilditch et al. 1996), in which "known" physical parameters for the components are adopted and used to calculate the resulting light curve, our modeling procedure makes no assumptions on component properties. Nevertheless, the use of previous measurements as the initial set of parameters for light curve modeling is useful for accelerating the fitting procedure. Moreover, once we know the amount of irradiation with respect to the average surface intensity of the secondary (I_s) and, assuming an irradiating energy, we can estimate the albedo of the star.

[3] We note that the model cannot separate the constant contribution of the primary from that of any other source, such as a shell or nebula, that may be contaminating the light from the system.

Table 5. Inferred parameters of TW Crv.

Fluxes of the different components:		
	J	H
F_2(mJy)	2.4 ± 0.6	2.1 ± 0.4
F_d(mJy)	17.8 ± 0.6	7.9 ± 0.3
I_{irr}	11.6 ± 0.2	6.3 ± 0.4
Simultaneouly fitted parameters:		
$i = (41 \pm 9)^\circ$ $q = (0.28 \pm 0.04)$ $f_{fac} = (1.13 \pm 0.01)$		

Table 6. Values for the albedo resulting from the light curve analysis.

	J	H	K_s
KV Vel	0.43 ± 0.04	0.44 ± 0.04	0.41 ± 0.04
TW Crv	0.6 ± 0.1	0.5 ± 0.1	–

For this analysis, the relation of I_s with the albedo can be derived from

$$\frac{T_1'}{T_1} = \sqrt[4]{R_t}, \qquad R_t = I_s = 1 + A_t \frac{F_s}{F_t}, \tag{4}$$

where T_1' is the modified effective temperature, T_1 is the local temperature at the stellar surface, R_t the local reflection factor, A_t the bolometric albedo, F_s the incident flux and F_t the undisturbed local flux (Kallrath & Milone 1999). By rearranging the terms in Eq. (4) we obtain

$$A_t = \frac{I_s - 1}{F_r}, \qquad \text{where} \qquad F_r = \frac{F_s}{F_t}. \tag{5}$$

We adopted our inferred radius of the secondary star and the values of Hilditch et al. (1996) and Chen et al. (1995) for the primary stars of KV Vel and TW Crv, respectively. We proceeded by considering that the primary and secondary stars in KV Vel have $T_1 = 77\,000$ K (Drilling 1985) and $T_2 = 3400$ K (Hilditch et al. 1996), respectively, and that they irradiate as black bodies[4]. With these assumptions we were able to calculate the emergent (F_t) and incident (F_s) flux at the surface of the star, and complete the calculations of Eq. (5). The results are listed in Table 6.

The resulting value for the albedo is strongly dependent on the assumed temperature for both stars. Therefore, in the case of TW Crv where the temperature of the primary is not constrained well, it is difficult to estimate the albedo reliably. The results in Table 6 were obtained by adopting a temperature for the primary of $T_1 = (105 \pm 20) \times 10^3$ K (Exter et al. 2005) and $T_2 = 4500$ K (Sect. 4.2) for the secondary.

Although the final value for the albedo still depends on the adopted temperature and irradiation field of both components (i.e. whether it is valid to approximate their radiation by a black body), we were able to provide a good fit to the data by adopting standard values for gravity- and limb-darkening, unlike the results of Hilditch et al. (1996). Further investigation of system parameters and details of the brightness distribution of the secondary are in demand for a better understanding of the system's properties and the physics of irradiated atmospheres.

[4] These assumptions are needed to provide a way to measure the incident and emergent flux at the surface of the secondary.

Acknowledgements. We would like to thank an anonymous referee for useful comments and suggestions, and Stella Kafka for a careful reading of an earlier version of the manuscript. This work was done with observations from the SOAR telescope, a partnership between CNPq-Brazil, NOAO, UNC, and MSU. T.R. acknowledges financial support from CAPES/CNPq through Ph.D. scholarship. R.B. acknowledges financial support from CNPq through grant 302.442/20088.

References

Baraffe, I., Chabrier, G., Allard, F., & Hauschildt, P. H. 1998, A&A, 337, 403
Chen, A., O'Donoghue, D., Stobie, R. S., et al. 1995, MNRAS, 275, 100
Claret, A. 1992, MNRAS, 335, 647
Drilling, J. 1985, ApJ, 294, 111
Exter, K. M., Pollacco, D. L., Maxted, P. F. L., Napiwotzki, R., & Bell, S. A. 2005, MNRAS, 359, 315
Han, Z., Podsiadlowski, P., Maxted, P. F. L., & Marsh, T. R. 2003, MNRAS, 341, 669
Hellier, C. 2001, Cataclysmic Variables Stars, 1st edn. (Chichester: Springer and Praxis)
Hilditch, R. W., Harries, T. J., & Hill, G. 1996, MNRAS, 279, 1380
Hilditch, R. W., Kilkenny, D., Lynas-Gray, A. E., & Hill, G. 2003, MNRAS, 344, 644
Kallrath, J., & Milone, E. F. 1999, Eclipsing Binary Stars, 1st edn. (Springer-Verlag)
Kilkenny, D., Spencer Jones, J., & Marang, F. 1988, Obs, 108, 88
Kolb, U., King, A. R., & Ritter, H. 1998, MNRAS, 298, 29
Kube, J., Gansicke, B. T., & Hoffmann, B. 2002, The Physics of Cataclysmic Variables and Related Objects, ASP Conf. Ser., 261
Landolt, A., & Drilling, J. 1986, AJ, 91, 1372
Pogge, R., Martini, P., & DePoy, D. 1999, OSU Astronomy
Press, W. H., Flannery, B. P., & Teukolsky, S. A. 1986 (Cambridge University Press)
Pringle, J. 1975, MNRAS, 170, 633
Ribeiro, T., Baptista, R., Harlaftis, E., Dhillon, V., & Rutten, R. 2007, A&A, 474, 213
Sarna, M. 1989, A&A, 224, 98
Schreiber, M. R., & Gänsicke, B. T. 2003, A&A, 406, 305
Skrutskie, M., Cutri, R., Stiening, R., et al. 2006, AJ, 131, 1163
Tappert, C., Gänsicke, B. T., Schmidtobreick, L., et al. 2007, A&A, 474, 205
Watson, C. 2002, PhD Thesis, Department of Physics and Astronomy, University of Sheffield
Wilson, R., & Devinney, E. J. 1971, ApJ, 166, 605